Received April 18, 2020, accepted May 5, 2020, date of publication May 19, 2020, date of current version June 4, 2020.

Digital Object Identifier 10.1109/ACCESS.2020.2995641

A Novel Mobile Target Localization Approach for Complicate Underground Environment in Mixed LOS/NLOS Scenarios

BO CAO[1,2], SHIBO WANG[1], SHIRONG GE[1], XIUZE MA[1], AND WANLI LIU[1]
[1]School of Mechatronic Engineering, China University of Mining and Technology, Xuzhou 221116, China
[2]School of Mechanic Engineering, Anhui Science and Technology University, Chuzhou 233100, China

Corresponding authors: Shibo Wang (wangshb@cumt.edu.cn) and Wanli Liu (4830@cumt.edu.cn)

This work was supported in part by the Joint Funds of the National Natural Science Foundation of China under Grant U1610251, Grant U51874279, and Grant 51974290, in part by the National Key Research and Development Program of China under Grant 2018YFC0604503, and in part by the Priority Academic Program Development (PAPD) of Jiangsu Higher Education Institutions.

ABSTRACT Accurate positioning of the shearer remains a challenge for automation of the longwall coal mining process. In this paper, the popular Ultra-wideband (UWB) positioning system that has attracted considerable attention is adopted to obtain the target node location. Unfortunately, localization accuracy is still unsatisfactory and unreliable in mixed line of sight (LOS) and non-line of sight (NLOS) scenarios. To ameliorate localization accuracy of UWB for complicate underground environment where the positioning scenarios suffered from frequently switching among LOS, NLOS, and mixed LOS-NLOS condition, the novel positioning algorithm GMM-IMM-EKF was proposed. Gaussian mixed model (GMM) was employed to re-estimate the measurement distance, and two parallel variational Bayesian adaptive Kalman filters (VBAKFs) under the structure of interacting multiple model (IMM) was utilized to smoothen the result of GMM to eliminate the LOS and NLOS errors, respectively. Then, the position of the target node was determined by exploiting extended Kalman filter (EKF) based on the outcome of IMM-VBAKF. The proposed approach was assessed by exploiting UWB P440 modules. Comparative experimental verification demonstrated that GMM-IMM-EKF strategy outperformed other positioning approaches, which can effectively reduce the adverse effect of NLOS errors and achieve higher positioning accuracy in underground environment with LOS/NLOS/LOS-NLOS transition conditions.

INDEX TERMS Ultra-wideband, variational Bayesian adaptive Kalman filter, Gaussian mixed model, interacting multiple model, underground environment.

I. INTRODUCTION

The shearer, a key equipment of a fully mechanized mining face (FMMF), played an important role in the coal production process. Monitoring of the shearer's position was of extreme significance for realizing the mining automation [1], [2]. The position and attitude of shearer can be usually determined by the inertial navigation positioning system (INS) or the inertial measurement units utilizing a combination of accelerometers and gyroscopes in the coal mine, which was because a global navigation satellite system was incapable for the underground environments [3]. When the pure inertial information was used in a free-inertial mode, the positioning error accumulated over time due to the typical drifting of the inertial sensor, albeit for a high-performance positioning system [4]. In order to obtain the higher localization accuracy of shearer, other positioning technologies have been utilized to assist the INS. Fortunately, the popular Ultra-wideband (UWB) technology, providing high accuracy on distance estimation and high-speed wireless data transmission, decreasing the effect of phenomena such as non-line-of-sight propagation and multipath [5], has enormous potential for the application of the underground environment.

To date, numerous researchers have conducted extensive studies on underground environment localization utilizing UWB positioning system. Yang *et al.* [6] proposed a stable INS/UWB integrated positioning system of the shearer using the multi-model intelligent switching method based on a tightly coupled integrated model and a decision tree fault-tolerant model. Qin *et al.* [7] studied a distributed

The associate editor coordinating the review of this manuscript and approving it for publication was Noor Zaman.

UWB-based localization system in the underground mines, and the distributed localization algorithm based on particle swarm optimization was proposed for underground mines and implemented on the blind node. Xie *et al.* [8] designed the UWB monitoring platform for underground localization to realize accurate and reliable positioning of the underground moving targets. Fan *et al.* [9] presented that the UWB positioning strategy for the shear was proposed to eliminate accumulative error produced by INS and the corresponding coupling model was established. Results demonstrated that the position of the shearer can be real-timely tracked by integrated positioning strategy, and positioning precision met the demand of actual working condition. Unfortunately, above mentioned approaches of target localization in line of sight (LOS) condition were difficult to yield satisfactory accurate position estimation and generated unreliable final estimation results due to non-line of sight (NLOS) error.

The surface and architecture of underground mine were usually irregular, and the FMMF kept dynamically changing frequently, making the signal propagation fall into reflection, diffraction, and scattering, which were referred to as NLOS paths. When the signal transmission channel between target node and anchor nodes (ANs) was in NLOS scenario, the measured distance was larger than that of LOS measurement due to the fact that the signal travelled longer path or time than direct link, causing additional positive bias which was called NLOS error. To handle with the NLOS error and enhance the positioning accuracy, NLOS error identification and NLOS error elimination were usually regarded as the two major approaches to deal with NLOS error. The NLOS identification attempted to distinguish between LOS and NLOS conditions, and was commonly based on range estimates [10], [11] or on the channel impulse response [12]–[14]. For the case of NLOS error elimination, several related approaches have been proposed to alleviate the adverse impact of NLOS measurement error. Chen [15] developed an algorithm to mitigate the NLOS errors by residual weighting when the range measurements corrupted by NLOS errors were not identifiable. Yu and Guo [16] proposed the Taylor-series-based weighted least squares algorithm under the assumption of knowledge of NLOS measurements. Li and Zhang [17] proposed that the coordinate's position obtained in the joint positioning were estimated as unscented Kalman filter (UKF) algorithm observations, and the measurement of the UKF update equation was modified, so that the algorithm can adapt the localization of NLOS environment. García *et al.* [18] took full advantage of the skewness of the estimated channel impulse response as a parameter to detect the NLOS condition and the extended Kalman filter (EKF) for accurate positioning in harsh environments. Shao *et al.* [19] proposed that the Kalman filter (KF) was used to eliminate the random NLOS delay caused by irregular devices, and then the parameter fitting and geometric method was employed to restrain the errors caused by the fixed NLOS delay in the locating area.

Underground environment was comparatively complicate and should be taken into consideration owing to the presence of obstructions such as hydraulic support, rough roadway walls, equipment, and moving pedestrians. When the mobile target moved along the FMMF, the propagation conditions inevitably changed between LOS and NLOS (LOS-NLOS) alternatively over the passing time. The frequently switching LOS and NLOS condition would cause serious measurement error for distance estimation, which was due to the fact that the measurement error characteristics varied for the case of LOS, NLOS, and LOS-NLOS, making the traditional NLOS positioning algorithm incapable to satisfy the requirements of underground localization only considering the single LOS or NLOS conditions. Consequently, in this paper, to reduce the measurement error and enhance the localization accuracy, a novel localization approach framework was proposed to handle with the dynamically changing propagation channel between ANs and the moving target node for underground environment with frequent transition of LOS/NLOS/LOS-NLOS scenarios. The main contributions of this study were exhibited as following:

(1) We proposed a novel approach to deal with the frequently changing propagation channel among LOS, NLOS and LOS-NLOS scenarios for the underground environment.

(2) We used the GMM-based algorithm for calculating the initial state probabilities of the LOS and NLOS condition, and eliminating the interference of LOS-NLOS situation, which was beneficial to obtain the more accurate measured distances between the target node and corresponding AN.

(3) Based on IMM structure, we employed two parallel VBAKFs smoothening the result of GMM to alleviate the LOS and NLOS errors, respectively, and then the more accurate distances estimation were acquired. Subsequently, we conducted comparative experiments to demonstrate the superiority of the proposed algorithm. Experimental results manifested that the NLOS error and localization accuracy can be significantly ameliorated with high robustness.

II. RELATED WORKS

Generally speaking, the more accurate ranging quality, the higher positioning accuracy. To enhance the measurement distance quality, in [20], a Gaussian Mixture Model (GMM) was proposed to re-estimate the measurement distance by considering the different Gaussian components with respect to LOS and NLOS ranging estimation, which has been demonstrated that the GMM approach has the ability of filtering NLOS errors from a set of NLOS corrupted range estimations. Qing *et al.* [21] adopted GMM algorithm to describe the LOS and NLOS propagation effects in order to overcome the problem of LOS and NLOS propagation identification in existing approaches. Zhang *et al.* [22] propounded that both ranging measurement and step length estimation were modeled using GMM, and one maximum likelihood estimator was developed. However, the GMM approach may

underestimate the true distance if there existed few NLOS measured distance [20].

On the other hand, to achieve the mobile target node localization in the mixed with LOS and NLOS conditions, KF [23], EKF [24], UKF [17], particle filters (PF) [25], and cubature Kalman filter (CKF) [26] were proposed to reduce the NLOS error. These algorithms can be applied to track a mobile target in non-stationary random processes, but they required a specific localization parameter at varying time points, and meanwhile became non-convergent in some circumstances [27]. The variational Bayesian [28] (VB)-based filtering estimators have been extensively adopted in the state estimation problem in the presence of unknown measurement noise. In [29] a VB adaptive Kalman filter (VBAKF) was proposed to jointly estimate the state and variances of the measurement noise. In [30] a modified VB noise adaptive KF was developed by designing a novel dynamic model for tracking the variances of measurement noise. Huang *et al.* [31] used the KF for LOS measurement distance filtering, and the modified VB approximation adaptive KF was proposed for NLOS condition filtering to estimate the mean and measurement noise covariance to eliminate the influence of NLOS.

However, due to the frequent transformation LOS and NLOS, the performance of the positioning system was weak, indicating that a single filter was insufficient to obtain the more accurate position. The interacting multiple model (IMM) algorithm has been demonstrated as one of the most effective approaches for estimation in dynamic system under uncertain environmental conditions [32]. Employing IMM algorithm exhibited better positioning performance than that of single dynamic model [33]. The IMM with different filter approaches such as KF, EKF, PF, CKF, UKF, and the hidden Markov models were utilized to realize the mobile location estimation. Xiang and Zhou [34] presented an interactive multiple model of UKF to estimate the target state in parallel to address target tracking in mixed LOS/NLOS condition, and the average consensus was employed to estimate global information contribution through information interaction between neighbors. Chen *et al.* [35] put forward that the combining EKF with the IMM scheme was used to smooth range estimation between the corresponding base station and mobile station in the rough wireless environment to mitigate the NLOS effects on the measurement error. Zhang *et al.* [36] proposed IMM-EKF algorithm that two KFs were adopted in parallel to accurately smoothen the distance measurement and meanwhile the EKF method was utilized to estimate the target's location, which was able to adapt the dynamically changing condition between LOS and NLOS due to the two KFs' interaction so that large NLOS ranging errors are further reduced. Chang and Fang [37] proffered the EKF and PF along with a three-model IMM algorithm were utilized and compared for mobile station tracking, and the result showed that the IMM-PF algorithm outperformed the IMM-EKF algorithm. Fritsche *et al.* [38] proposed that the IMM-EKF method was capable of coping with LOS and NLOS conditions modeled by employing a two-state Markov chain, where the LOS and NLOS errors were described by different noise models.

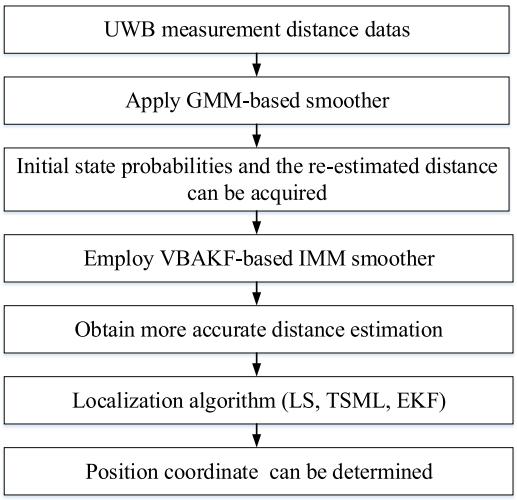

FIGURE 1. Localization algorithm flow chart.

The aforementioned localization approaches based on IMM estimation commonly required to set a fixed value for the initialization of state probability. Simultaneously, the above researchers usually concentrated on the transmission channels between the target node and ANs under the LOS and NLOS situations, easily ignoring the influence of the mixed LOS-NLOS condition when the surrounding environment was more complicate and changeable, such as the underground mine environment, causing to the lower precision and lower effectiveness during the process of localization. To bridge the above-mentioned research gap and achieve satisfactory positioning result for underground environment, in this paper, the novel algorithm framework for mobile localization was proposed by considering the problem of the constant initial state probability and the propagation conditions for LOS, NLOS, and LOS-NLOS scenarios. More specifically, we employed the GMM-based approach to eliminate the effect of LOS-NLOS situation on distance estimation so that the communication channel switched between LOS and NLOS scenarios and the initial state probability can be obtained for LOS and NLOS conditions, respectively. Subsequently, a VBAKF-based IMM framework, using the estimated state probabilities based on the GMM result and a Markov process with two interactive modes involvement LOS and NLOS conditions, was introduced to smooth the distance in order to obtain the higher ranging quality. Finally, EKF algorithm was adopted to calculate the target's position according to the smoothed result of VBAKF-based IMM method. To further verify the outstanding performance of the proposed method, the least square (LS) and two-stage Maximum Likelihood (TSML) approaches were executed to compute the target's position. According to the aforementioned description, the proposed positioning algorithm flow chart of this paper was depicted in Fig.1.

III. BACKGROUND AND GAUSSIAN MIXTURE MODEL

A. RECEIVED MEASUREMENTS

The actual distance donated by r_i between the target node and the ith AN is described as follows:

$$r_i = \sqrt{(x - x_i)^2 + (y - y_i)^2 + (z - z_i)^2} \tag{1}$$

The measurement distance between the target node and the i th AN for LOS can be expressed as:

$$\hat{d}_i^{los} = r_i + v_i \tag{2}$$

where v_i is the measurement noise obeyed a Gaussian distribution with zero mean and variance σ_{los}^2. In NLOS condition, due to the presence of obstacles in the direct path, the signal requires to be reflected and refracted to reach the ANs, so that the signal propagation path is increased, resulting in measurement distance larger than true distance. Thus, measurement distance is given by:

$$\hat{d}_i^{nlos} = r_i + v_i + b_{nlos}^i \tag{3}$$

where v_i is modeled as Gaussian distribution with zero mean and σ_{los}^2 variance. The NLOS error b_{nlos}^i is assumed to be independent, which is usually considered to obey the Gaussian distribution $N(\mu_b, \sigma_b^2)$.

Thus, the ranging error can be expressed as following:

$$\delta_i = \begin{cases} v_i & \text{LOS} \\ v_i + b_{nlos}^i & \text{NLOS} \end{cases} \tag{4}$$

The corresponding probability density function with respect to ranging error δ_i for LOS and NLOS conditions, respectively, can be expressed as the following form:

$$p^{los}(\delta_i) = \frac{1}{\sqrt{2\pi\sigma_{los}^2}} \exp\left(-\frac{\delta_i^2}{2\sigma_{los}^2}\right) \tag{5}$$

$$p^{nlos}(\delta_i) = \frac{1}{\sqrt{2\pi(\sigma_{los}^2 + \sigma_b^2)}} \exp\left(-\frac{(\delta_i - \mu_b)^2}{2(\sigma_{los}^2 + \sigma_b^2)}\right) \tag{6}$$

The measurement error can be modeled as a mixture Gaussians distribution in mixed LOS-NLOS condition, in which the distributions of LOS and NLOS measurement errors are represented by various Gaussian components.

B. RECEIVED MEASUREMENTS GMM FILTER

Without loss of generality, let d_m=$\{d_m^1, d_m^2, d_m^3, \ldots d_m^K\}$ donate the data set of K sample distance estimates between target node and the mth AN. For the LOS distance estimation, the probability density function of the measurement distance was commonly modeled as a Gaussian distribution [39], namely, $f_{los}(d_m) \sim N(r_{los}, \sigma_{los}^2)$, where r_{los} donates the true distance, σ_{los}^2 is of LOS variance. Meanwhile, it has been proved that the measured distance in NLOS scenario still obeyed a Gaussian distribution, $f_{nlos}(d_m) \sim N(r_{nlos}, \sigma_{nlos}^2)$[39], where $r_{nlos} = r_{los} + b_{nlos}$. Thereby, the GMM method was proposed to characterize the effects of LOS /NLOS/LOS-NLOS in this paper so as to more accurately describe the influence of the realistic underground environment, and the N-order GMM probability density function of measured distance d_m can be expressed as:

$$\begin{aligned} f(d_m; \theta_m) &= u_{m,1} f_{los} + \sum_{n=2}^{N} u_{m,n} f_{nlos,n} \\ &= \sum_{n=1}^{N} u_{m,n} \Theta(d_m; r_{m,n}, \sigma_{m,n}) \end{aligned} \tag{7}$$

where

$$\Theta(d_m; r_{m,n}, \sigma_{m,n}) = \frac{u_{m,\,n}}{\sqrt{2\pi}\sigma_{m,n}} \exp\left(-\frac{(d_m - r_{m,n})^2}{2\sigma_{m,n}^2}\right)$$

donates the Gaussian probability distribution of each sub-distribution; $u_{m,n}$ donates a mixed weight which satisfies $\sum_{n=1}^{N} u_{m,n} = 1$; $r_{m,n}$ is the distance between the target node and ANs, and it is the mean of each GMM components; $\sigma_{m,n}$ stands for the standard deviation; N denotes the total number of types of different error distributions, including LOS error and varying intensity of NLOS error. The model of probability density function can be successfully established based on appropriately selecting the component of the GMM, setting the suitable mixed weights, means and covariances, which can achieve a smooth approximation to the probability density function of the measured distance.

All measurement distances between the target node and the mth AN can be categorized by quite different Gaussian distributions allocated certain probabilities, and the centers of each category were the mean of Gaussian distribution, and the covariance matrix was considered as the corresponding dispersion. The parameter estimation of GMM components can be obtained by a given set of measurement distance according to a certain criterion, so that the determined GMM can best describe the probability distribution of the distance. To estimate the GMM components ($u_{m,n}$, $r_{m,n}$ and $\sigma_{m,n}$), the expectation maximization (EM) algorithm was applied to perform effectively parameter estimation, which was defined as an iterative two step algorithm for finding the optimal parameter that maximize the log likelihood function [40]. The involvement related parameters of iterative process of EM estimation, mixing probabilities $u_{m,n}$, means $r_{m,\text{n}}$, and standard deviations $\sigma_{m,n}$ are given by:

$$u_{m,n} = \frac{1}{K} \sum_{k=1}^{K} u_m(n\,|k\,) \tag{8}$$

$$r_{m,n} = \frac{\sum_{k=1}^{K} u_m(n\,|k\,) d_{m,k}}{\sum_{k=1}^{K} u_m(n\,|k\,)} \tag{9}$$

$$\sigma_{m,n} = \sqrt{\frac{\sum_{k=1}^{K} u_m(n\,|k\,)(d_{m,k} - r_{m,n})(d_{m,k} - r_{m,n})^T}{\sum_{k=1}^{K} u_m(n\,|k\,)}} \tag{10}$$

where $u_m(n\,|k\,)$ indicates the posteriori probability, expressed as follows:

$$u_m(n\,|k\,) = \frac{u_{m,n}\Theta(d_m; r_{m,n}, \sigma_{m,n})}{\sum_{i=1}^{N} u_{m,i}\Theta(d_m; r_{m,i}, \sigma_{m,i})} \tag{11}$$

Note that the aforementioned equations executed both the expectation step (E step) and the maximization step (M step) synchronously and iteratively updated E and M steps. The iteration stopped when the likelihood function achieved the maximum, then the GMM components parameters can be obtained. Thus, the initialization of GMM parameter, mainly including the mixed weight, average, covariance, and the number of categories, played a prominent role in increasing the precision of EM algorithm. As the EM algorithm was usually sensitive to the selection of the initial parameter, efficient initialization was significant preliminary process for the future convergence of the algorithm to the best global maximum of the likelihood function [41]. The inappropriate initial value made the EM algorithm easy fall into local maximum. K-means clustering was preferred for solving the initialization problem and provided better initial values. As a result, in this paper, to overcome the drawback of EM algorithm, K-means clustering was exploited to find the initial parameter value for an EM algorithm. Interested readers should consult the literature [42] for more details of involvement comprehensive description of the K-means clustering approach.

The measurement distance data can be distinguished LOS and NLOS measurement by using the K-means clustering algorithm when the measurement environment was subject to the mixed LOS/NLOS/LOS-NLOS scenarios, enabling the measurement condition only involve the LOS and NLOS ranges. The LOS distances can be estimated in LOS-NLOS condition by employing the proposed GMM-based method, therefore the ranging quality was improved by estimating the measured distance according to the Gaussian component of LOS estimations in GMM. Furthermore, the corresponding probabilities of LOS and NLOS measurement $(u_{m,1}, u_{m,2})$ with respect to AN_m can be obtained, which will be applied to compute the mixing probability for IMM smoother in the following section.

IV. VBAKF-BASED IMM SMOOTHER

A. STATE MODEL

The range state vector between AN_m and the target node at epoch $k+1$ is defined as follows:

$$D_m(k+1) = [d_m(k+1), \dot{d}_m(k+1)]^T \quad m = 1, 2, \ldots, M \quad (12)$$

where $d_m(k+1)$ and $\dot{d}_m(k+1)$ denotes the distance and the velocity of target node with regard to the mth AN, respectively, and M donates the number of the ANs. The measurement distance state-space model is represented as the following linear dynamic equation:

$$D_m(k+1) = FD_m(k) + Bw_d(k) \quad (13)$$

$$Z_m(k+1) = AD_m(k+1) + r(k+1) \quad (14)$$

where

$$F = \begin{bmatrix} 1 & T \\ 0 & 1 \end{bmatrix}, \quad B = \begin{bmatrix} T^2/2 \\ T \end{bmatrix},$$

and $A = [1, 0]$, T donates sample period; $w_d(k)$ donates the process noise [36], which is modeled as zero-mean Gaussian sequences with the covariance matrices Q; $r(k+1)$ represents the measurement noise whose covariance is $\hat{R}_k$ in mixed LOS/NLOS situation.

B. VBAKF ALGORITHM

In the conventional KF algorithm, the statistical moment of measurement noise was invariant and certain, enabling the performance of the traditional KF degrade because of the fact that in the actual environment the measurement noise might change with the time. The communication channel between the moving target node and corresponding AN was easily susceptible to affect by NLOS propagation condition due to the complex underground environment filled with large numbers of hydraulic supports and equipment, causing unknown and uncertain NLOS measurement noise. Hence, the VBAKF algorithm that can solve the estimation problem with unknown and time-varying measurement noise, was proposed to ameliorate the performance of AKF algorithm, by considering not only the change of noise, but also the variation of the predicted error covariance. The VBAKF was the combination of variational Bayesian (VB) and AKF; that was, measurement noise variances were approximated by VB, and system states were updated by AKF, which can estimate the measurement noise and system state. The VB approximation was a recursive approach that can approxi- mate the posterior distribution. Under the assumption that the dynamic models of the state and the noise covariance were mutually independent, the joint posterior probability density function with regard to the range state $D(k+1)$ and the measurement noise covariance $\hat{R}(k)$ at epoch $k+1$ can be expressed as following [26],

$$p(D(k+1), \hat{R}(k+1) \,|\, D(k), \hat{R}(k)) = p(D(k+1) \,|D(k))p(\hat{R}(k+1) \,|\, \hat{R}(k)) \quad (15)$$

Then, the VB approximation of the free-form is utilized to approximate the joint filtering distribution of the state and covariance matrix, expressed as following:

$$p(D(k+1), \hat{R}(k+1) \,|Z(k+1\,|k+1)) \approx Q(D(k+1))Q(\hat{R}(k+1)) \quad (16)$$

where $Q(D(k+1))$ and $Q(\hat{R}(k+1))$ indicate the unknown approximating densities. The VB-approximation can be executed by minimizing the Kullback-Leibler divergence between the approximation part $Q(D(k+1))Q(\hat{R}(k+1))$ and the true posterior $p(D(k+1), \hat{R}(k+1) \,|Z(k+1\,|k+1))$, given by:

$$\mathrm{KL}[Q(D(k+1))Q(\hat{R}(k+1)) \,\|\, p(D(k+1), \hat{R}(k+1) \,|Z(k+1\,|k+1))] = \int \log\left(\frac{Q(D(k+1))Q(\hat{R}(k+1))}{p(D(k+1), \hat{R}(k+1) \,|Z(k+1\,|k+1))}\right) \times Q(D(k+1))Q(\hat{R}(k+1))dD(k+1)d\hat{R}(k+1) \quad (17)$$

Thus, the minimum of KL divergence with regard to the probability densities $Q(D(k+1))$ and $Q(\hat{R}(k+1))$, respectively, can be obtained by remaining the other part fixed [43], expressed as following:

$$\begin{aligned} &Q(D(k+1)) \\ &\propto \exp\Big(\int \log p(Z(k+1), D(k+1), \hat{R}(k+1)\,|Z(k+1|\,k)) \\ &\quad \times Q(\hat{R}(k+1))d\hat{R}(k+1\,)) \end{aligned} \tag{18}$$

$$\begin{aligned} &Q(\hat{R}(k+1)) \\ &\propto \exp\Big(\int \log p(Z(k+1), D(k+1), \hat{R}(k+1)\,|Z(k+1\,|k\,)) \\ &\quad \times Q(D(k+1))dD(k+1\,)) \end{aligned} \tag{19}$$

The above coupled equations cannot be solved directly, nevertheless, the integrals in the exponentials of equation (18) and (19) can be expanded, respectively, expressed as follows:

$$\begin{aligned} &\int \log p(Z(k+1), D(k+1), \hat{R}(k+1) \\ &\quad \Big|Z(k+1\,|k\,))Q(\hat{R}(k+1))d\hat{R}(k+1) \\ &= -\frac{1}{2}(Z(k+1) - F(k+1)D(k+1))^T \left\langle (\hat{R}(k+1))^{-1} \right\rangle_{\hat{R}} \\ &\quad \times (Z(k+1) - F(k+1)D(k+1)) \\ &\quad -\frac{1}{2}(D(k+1) - \hat{D}(k+1\,|k\,))^T (P(k+1\,|k\,))^{-1} \\ &\quad \times (D(k+1) - \hat{D}(k+1\,|k\,)) + C_1 \end{aligned} \tag{20}$$

$$\begin{aligned} &\int \log p(Z(k+1), D(k+1), \hat{R}(k+1) \\ &\quad |Z(k+1\,|k\,))Q(D(k+1))dD(k+1\,) \\ &= -\sum_{i=1}^{m} (\frac{3}{2} + \alpha_{k+1,i}) \ln(\sigma_{k+1,i}^2) - \sum_{i=1}^{m} \frac{\beta_{k+1,i}}{\sigma_{k+1,i}^2} \\ &\quad -\frac{1}{2}\sum_{i=1}^{m} \frac{1}{\sigma_{k+1,i}^2} \left\langle (Z(k+1) - F(k+1)D(k+1))_i^T (Z(k+1) \right. \\ &\quad \left. -F(k+1)D(k+1))_i \right\rangle_D + C_2 \end{aligned} \tag{21}$$

where $\langle\cdot\rangle_D = \int(\cdot)Q(D(k+1))dD(k+1)$, $\langle\cdot\rangle_{\hat{R}} = \int(\cdot)Q(\hat{R}(k+1))d\hat{R}(k+1)$ and C_1, C_2 denotes constant values.

According to the relevant literature [29], the probability densities $Q(D(k+1))$ and $Q(\hat{R}(k+1))$ subjected to a Gaussian and inverse Gamma distribution, respectively, which can be represented as following:

$$Q(D(k+1)) = N(D(k+1); \hat{D}(k+1), P(k+1)) \tag{22}$$

$$Q(\hat{R}(k+1)) = \prod_{i=1}^{m} Inv - Gamma(\sigma_i^2\,|\alpha_i,\ \beta_i) \tag{23}$$

According to the reference [29], the parameters of equation (23) can be described as following:

Prediction:

$$\alpha_i(k+1\,|k\,) = \rho\alpha_i(k) \tag{24}$$

$$\beta_i(k+1\,|k\,) = \rho\beta_i(k) \tag{25}$$

Update:

$$\alpha_i(k+1) = 0.5 + \alpha_i(k+1\,|k\,) \tag{26}$$

$$\beta_i(k+1) = \beta_i(k+1\,|k\,) \tag{27}$$

where ρ donates a change factor in (0, 1]. The ranging noise covariance matrix can be expressed as follows:

$$\hat{R}_i(k+1) = diag\left(\frac{\beta_1^{(i)}(k+1)}{\alpha_1^{(i)}(k+1)}, \ldots, \frac{\beta_m^{(i)}(k+1)}{\alpha_m^{(i)}(k+1)}\right) \tag{28}$$

Iterate the following update equations with respect to the residual covariance $S_i(k+1)$, Kalman gain $G_i(k+1)$, ranging residual $V_i(k+1)$, state estimate $\hat{D}_{i+1}(k+1\,|k+1\,)$, covariance $P_{i+1}(k+1\,|k+1\,)$ and parameter $\beta_{i+1}(k+1)$, say N, steps are set as $i = 0,\ldots, N$, expressed as following:

$$S_i(k+1) = AP_i(k+1\,|k\,)A^T + \hat{R}_i(k+1) \tag{29}$$

$$G_i(k+1) = P_i(k+1\,|k\,)A^T S_i(k+1)^{-1} \tag{30}$$

$$V_i(k+1) = Z_i(k+1) - A\hat{D}_i(k+1\,|k\,) \tag{31}$$

$$\hat{D}_{i+1}(k+1\,|k+1\,) = \hat{D}_i(k+1\,|k\,) + G_i(k+1)V_i(k+1) \tag{32}$$

$$P_{i+1}(k+1\,|k+1\,) = P_i(k+1\,|k\,) - G_i(k+1)AP_i(k+1\,|k\,) \tag{33}$$

$$\begin{aligned} \beta_{i+1}(k+1) = \beta_i(k+1\,|k\,) + 0.5[(Z_i(k+1) \\ -\hat{D}_{i+1}(k+1))^2 + (AP_{i+1}(k+1\,|k \\ +1\,)A^T)_{ii}] \end{aligned} \tag{34}$$

where ii indicates diagonal elements of the matrix.

C. DISTANCE FILTERING BASED ON IMM APPROACH

The single filtering model was insufficient to smooth the estimated distances obtained from the output of the GMM method effectively due to the quite different measurement errors between LOS and NLOS scenarios. Consequently, IMM architecture algorithm that employed two parallel self-adjusting VBAKFs to smoothen the distance measurement errors with respect to LOS and NLOS conditions separately, was put forward to re-estimate the measured distance to generate higher precision ranging distance between the target node and the corresponding AN. When the target node mounted on the shearer moved along the scraper conveyor direction, the communication environment between the target node and ANs frequently alternated between LOS and NLOS which can be considered as a Markov process with two interactive modes due to the harsh underground environment. Markov chain consisted of two states, as depicted in Fig.2. Here, we let i and j ($i, j = 1, 2$) represent the mode variable, where $i, j = 1$ donates the LOS mode, and $i, j = 2$ donates the NLOS mode. The transition probabilities p_{ij} represents the conditional probability of states transition from state i at epoch k to state j at epoch $k+1$. $D_i(k)$ represents the input of the state mode i at epoch k. The state mode at epoch $k+1$ can be updated according to the following rule:

$$D_1(k+1) = \lambda_{11} \cdot D_1(k) + \lambda_{21} \cdot D_2(k) \tag{35}$$

$$D_2(k+1) = \lambda_{12} \cdot D_1(k) + \lambda_{22} \cdot D_2(k) \tag{36}$$

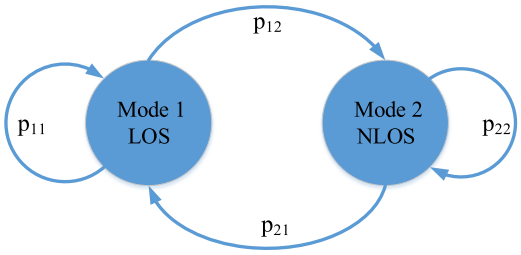

FIGURE 2. Markov switching chain for LOS/NLOS scenarios.

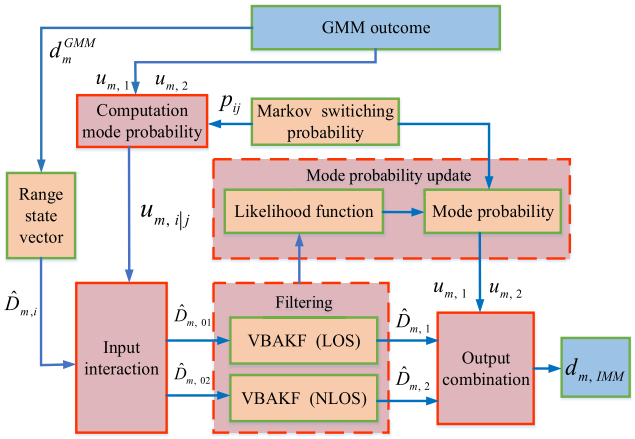

FIGURE 3. The architecture of VBAKF-IMM algorithm.

FIGURE 4. UWB P440 module.

where $\lambda_{11} = p_{11}/(p_{11}+p_{21})$, $\lambda_{21} = p_{21}/(p_{11}+p_{21})$, $\lambda_{12} = p_{12}/(p_{12}+p_{22})$, and $\lambda_{22} = p_{22}/(p_{12}+p_{22})$, which are the normalized transition probabilities, and p_{ij} satisfies the relations: $p_{11}+p_{12}=1$ and $p_{22}+p_{21}=1$.

The proposed VBAKF-based IMM smoother mainly consisted of five steps: computation the mode probability, input interaction, mode-matched filtering, mode probability update, and output combination, as shown in Fig. 3.

1) COMPUTATION THE MODE PROBABILITY

The mixing probability is calculated as:

$$u_{m,i|j}(k+1\,|k) = \frac{p_{ij}u_{m,i}(k)}{\bar{b}_{m,j}} \tag{37}$$

where p_{ij} donates the state transition probability, and $\bar{b}_{m,j}$ donates the normalized mode probability, which can be computed according to the following equation:

$$\bar{b}_{m,j} = \sum_{i=1}^{2} p_{ij}u_{m,i}(k) \tag{38}$$

2) INPUT INTERACTION

The initial condition of the state vectors $\hat{D}_{m,0j}(k+1\,|k)$ and the corresponding covariance matrices $P_{m,0j}(k+1\,|k)$ can be calculated for the jth mode-match filter of mth AN based on the input mixing probabilities, respectively, which can be expressed as following:

$$\hat{D}_{m,0j}(k+1\,|k) = \sum_{i=1}^{2} u_{m,\,i|j}(k+1\,|k)\hat{D}_{m,i}(k\,|k) \tag{39}$$

$$\begin{aligned} P_{m,0j}(k+1\,|k) = &\sum_{i=1}^{2} u_{m,i|j}(k+1\,|k) \times \{P_{m,i}(k\,|k) \\ &+[\hat{D}_{m,i}(k\,|k) - \hat{D}_{m,0j}(k+1\,|k)] \\ &\times[\hat{D}_{m,i}(k\,|k) - \hat{D}_{m,0j}(k+1\,|k)]^T\} \end{aligned} \tag{40}$$

3) MODE-MATCHED FILTERING

The two parallel VBAKFs were utilized to filter the distance, which was due to the fact that the measurement noise were completely different between LOS and NLOS scenarios. One VBAKF was formulated to filter the LOS measured distance and another was designed to smoothen the NLOS ranges. According to the above descriptions, the two mode-matched VBAKFs were running simultaneously, and the entire filtering procedure of the VBAKF was presented as following:

4) MODE PROBABILITY UPDATE

According to the innovation vector $V_{m,j}(k+1)$ and its corresponding covariance $S_{m,j}(k+1)$, the likelihood function for filter j can be computed as follows:

$$\begin{aligned} \Lambda_{m,j}(k+1) = &\frac{1}{\sqrt{2\pi\,|S_{m,j}(k+1)|}} \\ &\times \exp\left(\frac{V_{m,j}^T(k+1)V_{m,j}(k+1)}{2S_{m,j}(k+1)}\right) \end{aligned} \tag{41}$$

where $S_{m,j}(k+1) = HP_{m,j}(k+1\,|k)H^T + \hat{R}$

Then, the mode probability can be updated based on the likelihood values and transition probability, expressed as follows:

$$u_{m,j}(k+1) = \frac{\Lambda_{m,j}(k+1)\bar{b}_{m,j}}{b_m} \tag{42}$$

where $b_m = \sum_{i=1}^{2} \Lambda_{m,i}(k+1)\bar{b}_{m,i}$

Algorithm VBAKF algorithm

Prediction:

$$\begin{aligned}\hat{D}_{m,j}(k+1\,|k) &= F\hat{D}_{m,0j}(k+1\,|k)\\ P_{m,j}(k+1\,|k) &= FP_{m,0j}(k+1\,|k)F^T+\hat{R}\\ \alpha_i(k+1\,|k) &= \rho\alpha_i(k)\\ \beta_i(k+1\,|k) &= \rho\beta_i(k)\end{aligned}$$

Update: First set

$$\begin{aligned}\hat{D}^{(0)}_{m,j}(k+1\,|k) &= \hat{D}_{m,j}(k+1\,|k),\\ P^{(0)}_{m,j}(k+1\,|k) &= P_{m,j}(k+1\,|k)\\ \alpha_i(k+1) &= 0.5+\alpha_i(k+1\,|k),\\ \beta^{(0)}_i(k+1) &= \beta_i(k+1\,|k).\end{aligned}$$

Iterate the following until the convergence (say, N times for t = 1, 2, …, N)

$$\begin{aligned}\hat{R}^{(t)}(k+1) &= diag\left(\frac{\beta^{(t)}_1(k+1)}{\beta^{(t)}_1(k+1)},\ldots,\frac{\beta^{(t)}_m(k+1)}{\alpha^{(t)}_m(k+1)}\right)\\ S^{(t+1)}_{m,j}(k+1) &= AP_{m,j}(k+1\,|k)A^T+\hat{R}^{(t)}(k+1)\\ G^{(t+1)}_{m,j}(k+1) &= P_{m,j}(k+1\,|k)A^T\left(S^{(t+1)}_{m,j}(k+1)\right)^{-1}\\ V_{m,j}(k+1) &= \hat{d}_m(k+1)-A\hat{D}_{m,j}(k+1\,|k)\\ \hat{D}^{(t+1)}_{m,j}(k+1\,|k+1) &= \hat{D}_{m,j}(k+1\,|k)+G^{(t+1)}_{m,j}(k+1)\\ &\quad V_{m,j}(k+1)\\ P^{(t+1)}_{m,j}(k+1\,|k+1) &= P_{m,j}(k+1\,|k)-G^{(t)}_{m,j}(k+1)\\ &\quad AP_{m,j}(k+1\,|k)\\ \beta^{(t+1)}_i(k+1) &= \beta_i(k+1\,|k)+0.5[(Z_i(k+1)\\ &\quad -\hat{D}^{(t+1)}(k+1))^2\\ &\quad +(AP^{(t+1)}(k+1\,|k+1)A^T)_{ii}]\end{aligned}$$

and set

$$\begin{aligned}\beta_i(k+1) &= \beta^{(N)}_i(k+1),\\ \hat{D}_{m,j}(k+1\,|k+1) &= \hat{D}^{(N)}(k+1\,|k+1),\\ P_{m,j}(k+1\,|k+1) &= P^{(N)}_{m,j}(k+1\,|k+1)\end{aligned}$$

5) OUTPUT COMBINATION

The state estimation and error covariance estimation of the measured distance for each AN from the result of two mode-matched filters were combined with the respective mode probabilities to yield the final state estimate $\hat{D}_m(k+1\,|k+1)$ and covariance estimate $P_m(k+1\,|k+1)$, expressed as follows:

$$\begin{aligned}&\hat{D}_m(k+1\,|k+1)\\ &\quad=\sum_{i=1}^{2}u_{m,\,i}(k+1)\hat{D}_{m,i}(k+1\,|k+1)\end{aligned}\tag{43}$$

$$\begin{aligned}&P_m(k+1\,|k+1)\\ &\quad=\sum_{i=1}^{2}u_{m,i}(k+1)\times\{P_{m,i}(k+1\,|k+1)\\ &\qquad+[\hat{D}_{m,i}(k+1\,|k+1)-\hat{D}_m(k+1\,|k+1)]\\ &\qquad\times[\hat{D}_{m,i}(k+1\,|k+1)-\hat{D}_m(k+1\,|k+1)]^T\}\end{aligned}\tag{44}$$

Consequently, the final smoothed distance estimation for AN_m can be calculated from the estimation state vector $\hat{D}_m(k+1\,|k+1)$, expressed as follows:

$$d_{m,IMM}(k+1)=A\hat{D}_m(k+1\,|k+1)\tag{45}$$

V. LOCATION CALCULATION

A. LEAST SQUARE METHOD

The more accurate estimation of the measurement distances between the four individual ANs and target node can be obtained from the outputs utilizing the GMM method and VBAKF-based IMM smoother, and the location of the target node was calculated by the LS approach. According to the estimated distances $d_{m,IMM}(k+1)$, the TOA positioning model observation equations can be established as:

$$\begin{cases}(x(k+1)-x_1)^2+(y(k+1)-y_1)^2+(z(k+1)-z_1)^2\\ \quad=d^2_{1,IMM}(k+1)\\ (x(k+1)-x_2)^2+(y(k+1)-y_2)^2+(z(k+1)-z_2)^2\\ \quad=d^2_{2,IMM}(k+1)\\ (x(k+1)-x_3)^2+(y(k+1)-y_3)^2+(z(k+1)-z_3)^2\\ \quad=d^2_{3,IMM}(k+1)\\ (x(k+1)-x_4)^2+(y(k+1)-y_4)^2+(z(k+1)-z_4)^2\\ \quad=d^2_{4,IMM}(k+1)\end{cases}\tag{46}$$

where (x_i, y_i, z_i) donates the known coordinates of the anchor node i (i = 1, 2, 3, 4), and $(x(k+1), y(k+1), z(k+1))$ donates the position of the target node.

Equation (46) was transformed into a matrix form after some mathematical manipulation, written as:

$$AX=B\tag{47}$$

where

$$A=\begin{bmatrix}(x_2-x_1)&(y_2-y_1)&(z_2-z_1)\\(x_3-x_1)&(y_3-y_1)&(z_3-z_1)\\(x_4-x_1)&(y_4-y_1)&(z_4-z_1)\end{bmatrix},\ X=\begin{bmatrix}x(k+1)\\y(k+1)\\z(k+1)\end{bmatrix},$$

$$B=\frac{1}{2}\begin{bmatrix}a_2-a_1+d^2_{1,IMM}(k+1)-d^2_{2,IMM}(k+1)\\a_3-a_1+d^2_{1,IMM}(k+1)-d^2_{3,IMM}(k+1)\\a_4-a_1+d^2_{1,IMM}(k+1)-d^2_{4,IMM}(k+1)\end{bmatrix}\ \text{and}$$

$a_i=x_i^2+y_i^2+z_i^2$.

The least square solution of the target node can be obtained, expressed as following:

$$X=(A^TA)^{-1}A^TB\tag{48}$$

B. TWO-STAGE MAXIMUM LIKELIHOOD ALGORITHM

The TSML algorithm was a two-step method to obtain the location of the target node by employing the maximum likelihood approach, which has been proven that this method can achieve the Cramér-Rao lower bound for the position estimator [44]. To apply the TSML algorithm, the quadratic system of equations (48) can be written as the following form:

$$\begin{cases} -2x_1x(k+1)+y_1y(k+1)+z_1z(k+1)+s(k+1)=f_1 \\ -2x_2x(k+1)+y_2y(k+1)+z_2z(k+1)+s(k+1)=f_2 \\ -2x_3x(k+1)+y_3y(k+1)+z_3z(k+1)+s(k+1)=f_3 \\ -2x_4x(k+1)+y_4y(k+1)+z_4z(k+1)+s(k+1)=f_4 \end{cases} \tag{49}$$

where

$$f_1 = d^2_{1,IMM}(k+1)-a_1,\ f_2 = d^2_{2,IMM}(k+1)-a_2,$$
$$f_3 = d^2_{3,IMM}(k+1)-a_3,\ f_4 = d^2_{4,IMM}(k+1)-a_4, \text{ and}$$
$$s(k+1) = x^2(k+1)+y^2(k+1)+z^2(k+1).$$

Equation (49) can be converted into the matrix, given by:

$$Gv = h_1 \tag{50}$$

where

$$h_1 = \begin{bmatrix} d^2_{1,IMM}(k+1)-a_1 \\ d^2_{2,IMM}(k+1)-a_2 \\ d^2_{3,IMM}(k+1)-a_3 \\ d^2_{4,IMM}(k+1)-a_4 \end{bmatrix}, \quad v = \begin{bmatrix} x(k+1) \\ y(k+1) \\ z(k+1) \\ s(k+1) \end{bmatrix},$$

$$G = \begin{bmatrix} -2x_1 & -2y_1 & -2z_1 1 \\ -2x_2 & -2y_2 & -2z_2 1 \\ -2x_3 & -2y_3 & -2z_3 1 \\ -2x_4 & -2y_4 & -2z_4 1 \end{bmatrix}$$

The weighted least-square solution of equation (50) can be expressed as follows:

$$v = (G^T W_1 G)^{-1} G^T W_1 h_1 \tag{51}$$

where

$$W_1 = (4B^T QB)^{-1} \tag{52}$$

And Q represents a diagonal matrix whose diagonal entries are the variances computed from the smoothed distance. B donates a diagonal matrix whose entries are the smoothed distance from the result of IMM filter.

Then, the element of $\boldsymbol{v}$ can be expressed as:

$$\begin{cases} v_1 = x(k+1)+e_1(k+1) \\ v_2 = y(k+1)+e_2(k+1) \\ v_3 = z(k+1)+e_3(k+1) \\ v_4 = s(k+1)+e_4(k+1) \end{cases} \tag{53}$$

where $e_1(k+1)$, $e_2(k+1)$, $e_3(k+1)$ and $e_4(k+1)$ represent the estimated errors with regard to v.

Then, square $v_1(k+1)$, $v_2(k+1)$, $v_3(k+1)$ and the objective function with ψ as error vectors of w is constructed, which is expressed as follows:

$$\psi = h_2 - Mw \tag{54}$$

where

$$M = \begin{bmatrix} 1 & 0 & 0 \\ 0 & 1 & 0 \\ 0 & 0 & 1 \\ 1 & 1 & 1 \end{bmatrix},\ h_2 = \begin{bmatrix} v_1^2 \\ v_2^2 \\ v_3^2 \\ v_4 \end{bmatrix}, w = \begin{bmatrix} \hat{x}_1^2(k+1) \\ \hat{y}_2^2(k+1) \\ \hat{z}_3^2(k+1) \end{bmatrix}, \text{ and}$$

$$\psi = \begin{bmatrix} 2\hat{x}(k+1)e_1(k+1)+e_1^2(k+1) \\ 2\hat{y}(k+1)e_2(k+1)+e_2^2(k+1) \\ 2\hat{z}(k+1)e_3(k+1)+e_3^2(k+1) \\ e_4(k+1) \end{bmatrix}$$
$$\approx \begin{bmatrix} 2\hat{x}(k+1)e_1(k+1) \\ 2\hat{y}(k+1)e_2(k+1) \\ 2\hat{z}(k+1)e_3(k+1) \\ e_4(k+1) \end{bmatrix}$$

Then, the covariance matrix of the error vector ψ can be computed as follows:

$$\Phi = E(\psi\psi^T) = 4B_2^T(GW_1G)^{-1}B_2 \tag{55}$$

Then, the weighted least square solution of equation (54) that minimizes $\psi^T W_2 \psi$ to produce more accurate position estimate can be expressed as:

$$w(k+1) = (M^T W_2 M)^{-1} M^T W_2 h_2 \tag{56}$$

where W_2 represents a positive definite matrix [45], which is given by:

$$W_2 = [4B_2^T(GW_1G)^{-1}B_2]^{-1} \tag{57}$$

where B_2 donates the following diagonal matrix, expressed as follows:

$$B_2 = \begin{bmatrix} x(k+1) & 0 & 0 & 0 \\ 0 & y(k+1) & 0 & 0 \\ 0 & 0 & z(k+1) & 0 \\ 0 & 0 & 0 & 0.5 \end{bmatrix} \tag{58}$$

Because B_2 contains the true coordinate position of the target node, in practical scenarios the true value ($x(k+1)$, $y(k+1)$, $z(k+1)$) of the target is not available [46], which is replaced with their corresponding estimated values v_1, v_2, v_3. Thus, the desired estimate of the target coordinate position can be calculated as:

$$\begin{bmatrix} x(k+1) \\ y(k+1) \\ z(k+1) \end{bmatrix} = \begin{bmatrix} \sqrt{|w_1(k+1)|} \\ \sqrt{|w_2(k+1)|} \\ \sqrt{|w_3(k+1)|} \end{bmatrix} \tag{59}$$

C. EXTENDED KALMAN FILTER METHOD

Unlike the LS and TSML algorithms, the EKF aimed to cope with nonlinear issue aroused by the covariance of measured distance and dynamic localization problem of the target node, which can achieve position estimation in real-time by employing the information of the objective. The basic idea of EKF algorithm was to transform a nonlinear system into an approximate linear system based on the first-order Taylor series expansion. The main process of EKF positioning algorithm is designed as follows:

The state space vector of the target node representation of the form at epoch $k+1$ is given by:

$$X(k+1) = [x(k+1), \dot{x}(k+1), y(k+1), \dot{y}(k+1), z(k+1), \dot{z}(k+1)]^T \quad (60)$$

where $(x(k+1), y(k+1), z(k+1))$ and $(\dot{x}(k+1), \dot{y}(k+1), \dot{z}(k+1))$ respectively, donates the coordinate and velocity of the target node at epoch $k+1$.

The corresponding state model is given by:

$$X(k+1) = \Phi X(k) + Cv(k) \quad (61)$$

where

$$\Phi = \begin{bmatrix} 1 & T & 0 & 0 & 0 & 0 \\ 0 & 1 & 0 & 0 & 0 & 0 \\ 0 & 0 & 1 & T & 0 & 0 \\ 0 & 0 & 0 & 1 & 0 & 0 \\ 0 & 0 & 0 & 0 & 1 & T \\ 0 & 0 & 0 & 0 & 0 & 1 \end{bmatrix},$$

$$C = \begin{bmatrix} T^2/2 & 0 & 0 \\ T & 0 & 0 \\ 0 & T^2/2 & 0 \\ 0 & T & 0 \\ 0 & 0 & T^2/2 \\ 0 & 0 & T \end{bmatrix},$$

and $v(k)$ donates a white Gaussian process with zero-mean and covariance matrix Q. The observation equation can be considered as follows:

where (x_m, y_m, z_m) stands for the coordinate of mth AN, and $(x(k+1), y(k+1), z(k+1))$ donates the target node's estimation coordinate calculated from the equation (61). Extending the observation equation (62), as shown at the bottom of the next page, in Taylor series and ignoring the two powers and higher term, the matrix H can be constructed, expressed as follows:

$$H = \begin{bmatrix} h_{1,x} & 0 & h_{1,y} & 0 & h_{1,z} & 0 \\ h_{2x} & 0 & h_{2,y} & 0 & h_{2,z} & 0 \\ h_{3,x} & 0 & h_{3,y} & 0 & h_{3,z} & 0 \\ h_{4,x} & 0 & h_{4,y} & 0 & h_{4,z} & 0 \end{bmatrix} \quad (63)$$

where

$$h_{m,x} = \frac{\partial h_m(\hat{X}(k+1|k))}{\partial x(k+1|k)} = \frac{x(k+1) - x_m}{L_m},$$

$$h_{m,y} = \frac{\partial h_m(\hat{X}(k+1|k))}{\partial y(k+1|k)} = \frac{y(k+1) - y_m}{L_m},$$

$$h_{m,z} = \frac{\partial h_m(\hat{X}(k+1|k))}{\partial z(k+1|k)} = \frac{z(k+1) - z_m}{L_m}, \ m = 1, 2, 3, 4,$$

and

$$L_m = \sqrt{(x(k+1)-x_m)^2 + (y(k+1)-y_m)^2 + (z(k+1)-z_m)^2}$$

The key step of EKF approach can be executed as following:

1). *Predicted state estimate*

$$\hat{X}(k+1|k) = \Phi X(k|k) \quad (64)$$

2). *Predicted state error covariance*

$$\hat{P}(k+1|k) = \Phi P(k+1|k)\Phi^T + CQC^T \quad (65)$$

3). *Near-optimal Kalman gain*

$$G(k+1) = \hat{P}(k+1|k)H^T[H\hat{P}(k+1|k)H^T + HRH^T]^{-1} \quad (66)$$

4). *Updated state estimate*

$$X(k+1|k+1) = \hat{X}(k+1|k) + G(k+1)[D_m^{IMM}(k+1) - h_m(\hat{X}(k+1|k))] \quad (67)$$

where $D_{m,IMM}(k+1) = [d_{1,IMM}(k+1|k), \ldots, d_{m,IMM}(k+1|k)]^T$ donates the vector of estimated distance obtained from IMM filter.

5). *Updated state error covariance*

$$P(k+1|k+1) = \hat{P}(k+1|k) - G(k+1)H\hat{P}(k+1|k) \quad (68)$$

Based on aforementioned process, the EKF algorithm was utilized to predict and update the estimated position of the target node, which not only realized the location estimation of the moving target, but also further eliminate the influence of the residual distance error on the positioning accuracy after filtering the measurement distance by IMM method. The measurement errors caused by LOS, NLOS and LOS-NLOS have been diminished significantly by taking advantage of the combination of GMM filter and IMM-based smoother, which was beneficial to achieve relatively more accurate and reliable position estimation for the mobile target node in the mixed LOS/NLOS/LOS-NLOS scenarios.

VI. EXPEROMENTAL RESULT AND ANALYSIS

A. UWB P440 MODULE LOCALIZATION EXPERIMENT

The UWB P440 module, employing the two-way time of flight (TW-TOF) approach for ranging between two or more modules, and providing a bandwidth of 3.1-4.8 GHz and the center frequency of 4.3 GHz with the measurement accuracy up to 50 px and the refresh rate up to 125 Hz [47], was produced by the American time domain company, as shown in Fig. 4. Hence, we selected the UWB P440 modules as the target node and ANs. The target node was installed on the fuselage of shearer. Four ANs were deployed in the roadway at the end of the FMMF, and the shape of ANs was arranged into V-shape deployment configuration which was regarded as an excellent layout [48], as presented in Fig.5.

In order to verify the feasibility and effectiveness of the performance of the proposed positioning algorithm for the

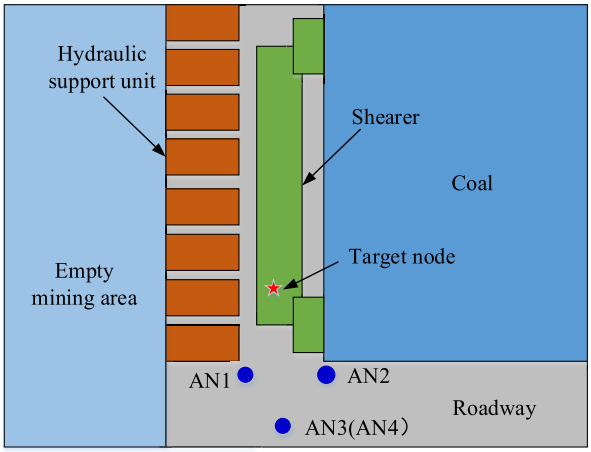

FIGURE 5. Schematic diagram of UWB sensors deployment in the end of the fully mechanized mining face.

FIGURE 6. UWB positioning system in the experiment environment.

mobile target node in this paper, the experiments were carried out in underground roadway Laboratory of China University of Mining and Technology, as depicted in Fig.6. There was a sampling point along the set trajectory of the mobile target node every 0.15 m and 500 measurements were collected for each sampling point. At each localization point, the staff moved backwards and forwards between the target node and ANs to collect a group of LOS-NLOS measured distance data during this process, as illustrated in Fig.7. The coordinates of four ANs were set as AN1 (5.436, 0.614, 0.843), AN2 (5.436, 4.821, 1.367), AN3 (6.945, 2.416, 1.857), AN4 (6.954, 2.416, 0.446), respectively, and the target node moved along a straight path. The two-state Markov transition probabilities were set as $p_{11} = 0.95$, $p_{12} = 0.05$, $p_{21} = 0.05$,

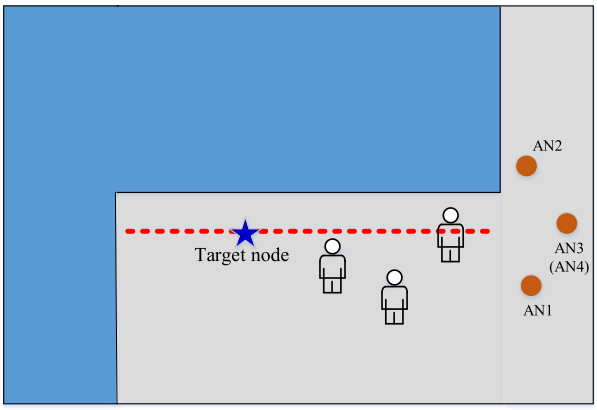

FIGURE 7. Schematic diagram of UWB sensor positioning experiment.

and $p_{22} = 0.95$. The measurement noise parameters in LOS and NLOS conditions can be acquired by offline test, with mean of LOS error $\mu_{los} = 0$, standard deviation of LOS error $\sigma_{los} = 0.04\ m$, mean of NLOS error $\mu_{nlos} = 0.08\ m$, and standard deviation of NLOS error $\sigma_{nlos} = 0.12\ m$.

B. MEASUREMENT DISTANCE ERROR ESTIMATION

The measurement distance between the target node and corresponding anchor node can be measured by using UWB P440 self-network. The localization algorithm can computed the target node's position. Nevertheless, if we directly used the average of measurement distance for localization in mixed LOS-NLOS scenario, larger positioning error occurred. For example, the measured distance data of anchor node AN1 at the localization point 6 under the LOS situation companied by the NLOS scenario due to the dynamic obstacles such as the moving people was depicted in Fig.8, revealing that the measured distances were effected by NLOS. If we only took into consideration the LOS scenario ignoring the NLOS existing in thus mixed LOS-NLOS situation, it would give rise to large errors for distance estimated by utilizing the mean of all measurement distance, which would produce unreliable positioning result. Consequently, we firstly adopted GMM method to smoothen the measured distance and computed the initial state probabilities of the LOS and NLOS scenarios, and then the VBAKF-based IMM was used to further improve the estimated distance quality of the result of the GMM.

For all localization points of AN1, the estimated distance error computed by using the mean directly, GMM and GMM-IMM methods were illustrated in Fig.9. It can be observed that GMM algorithm can effectively mitigate the error of measured distance and obtain the better ranging quality in the mixed LOS, NLOS, and LOS-NLOS situations. This was

$$\begin{aligned} z_m(k+1) &= h_m(\hat{X}(k+1\,|k\,)) \\ &= \sqrt{(x(k+1\,|k\,)-x_m)^2+(y(k+1\,|k\,)-y_m)^2+(z(k+1\,|k\,)-z_m)^2} \end{aligned} \tag{62}$$

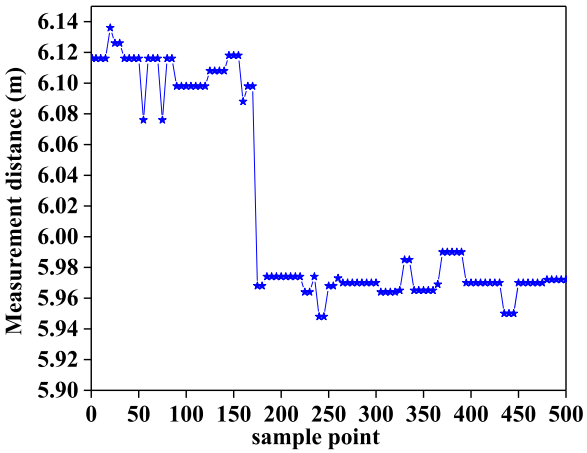

FIGURE 8. Measurement distance in mixed LOS and NLOS condition.

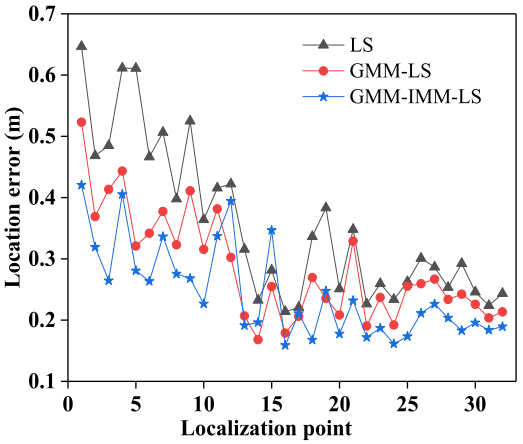

FIGURE 10. Comparison of location estimation error by utilizing LS, GMM-LS and GMM-IMM-LS positioning algorithms.

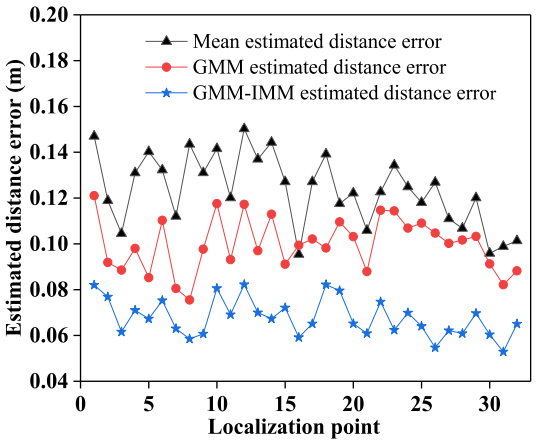

FIGURE 9. Estimated distance error computed by using mean directly, GMM and GMM-IMM approaches.

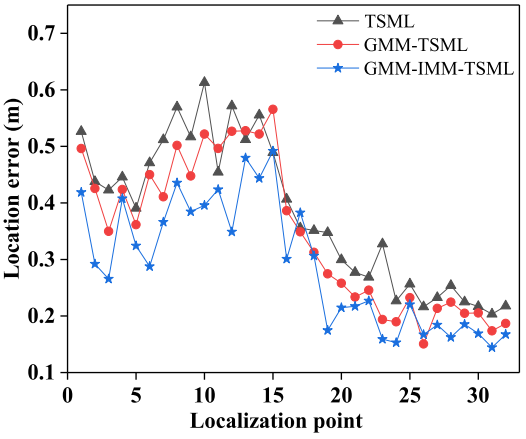

FIGURE 11. Comparison of location estimation error by utilizing TSML, GMM-TSML and GMM-IMM-TSML positioning algorithms.

because the GMM approach was capable to filter noise and NLOS error from the measured distances including LOS and NLOS measurement. After getting relatively accurate distances, the VBAKF-based IMM was executed based on the actual state probabilities of the LOS and NLOS scenarios from the GMM to further ameliorate the ranging quality. Compared with the techniques of using the mean to estimate distances directly and GMM, the more accurate distance with the lowest estimated distance error providing approximately 0.06 m∼0.08 m can be computed by using GMM-IMM. IMM technique had the self-adaptive feature with adjusting the probability of each model and combining with the weighted fusion estimation of LOS and NLOS distance, which was beneficial to further reduce the error of the estimated distance.

C. LOCALIZATION RESULT ANALYSIS

To overall assess the superiority of the proposed positioning algorithm, the root mean square error (RMSE) was usually used to evaluate the positioning error, expressed as follows:

$$RMSE = \sqrt{(x - x_r)^2 + (y - y_r)^2 + (z - z_r)^2} \quad (69)$$

where (x, y, z) donates the estimated location of the target node obtained by utilizing mentioned positioning algorithms, respectively, and (x_r, y_r, z_r) represents the real coordinate.

To demonstrate the effectiveness and superiority of the proposed GMM-IMM-EKF algorithm in this paper, different position computation methods with respect to LS and TSML under the framework of GMM-IMM algorithm were applied, respectively. Moreover, these methods were compared with the GMM-LS, GMM-TSML, GMM-EKF algorithm and their corresponding single-model localization algorithms to further understand the advantage of GMM-IMM technique.

The performance comparison with regard to the localization error of the target node employing the different algorithms was depicted in Figs.10-12. It was noted that, the single LS, TSML, and EKF algorithms provided higher localization error due to the influence of NOLS and mixed LOS-NLOS condition. Compared to the approaches of

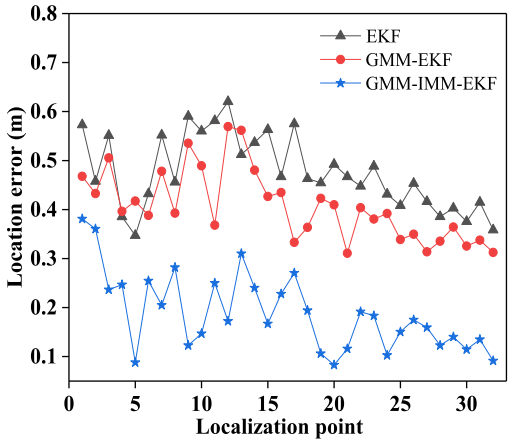

FIGURE 12. Comparison of location estimation error by utilizing EKF, GMM-EKF and GMM-IMM-EKF positioning algorithms.

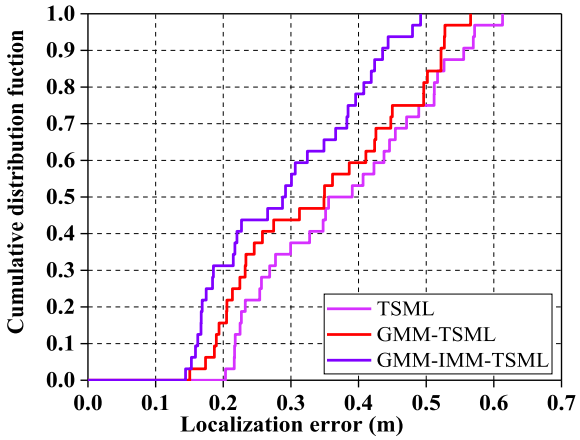

FIGURE 14. The cumulative distribution function of localization error by using TSML, GMM-TSML and GMM-IMM-TSML positioning algorithms.

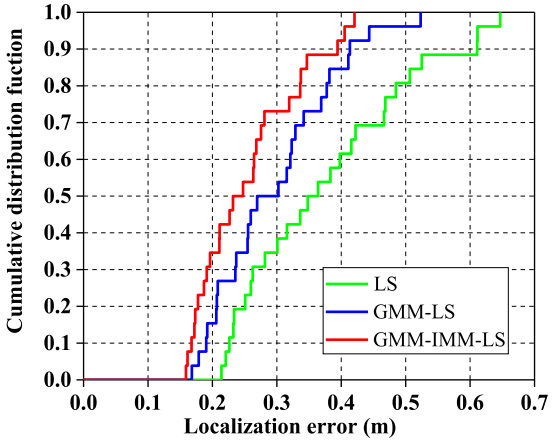

FIGURE 13. The cumulative distribution function of localization error by utilizing LS, GMM-LS and GMM-IMM-LS positioning algorithms.

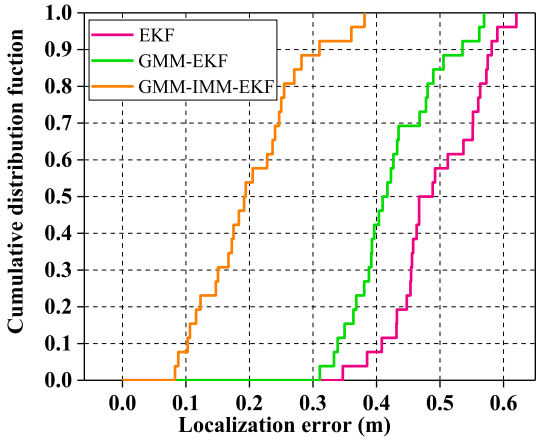

FIGURE 15. The cumulative distribution function of localization error by utilizing EKF, GMM-EKF and GMM-IMM-EKF positioning algorithms.

utilizing the average value to estimate distance, the estimation distance by utilizing GMM method got more accurate distance estimation because the GMM approach had the ability of filtering both noise and NLOS errors from a set of NLOS damaged measurement distances [21], which made the GMM-LS, GMM-TSML, and GMM-EKF algorithms more accurate in terms of localization accuracy than that of single positioning algorithm LS, TSML, together with EKF. Synchronously, the GMM-IMM-LS, GMM-IMM-TSML and GMM-IMM-EKF approaches can tremendously diminish localization errors and achieve better positioning accuracy by introducing the result of two different parallel self-adjusting VBAKFs for LOS and NLOS condition into the weighted fusion estimation in the IMM structure compared with the GMM-LS, GMM-TSML and GMM-EKF, respectively. Furthermore, the localization error of the GMM-IMM-EKF algorithm was much smaller than that of GMM-IMM-LS and GMM-IMM-TSML methods, exhibiting the best positioning performance and robustness.

The cumulative distribution function (CDF) of localization errors obtained in the evaluation scenario with different localization algorithms were presented in Figs.13-15. It was straightforward to observe that, for the LS, GMM-LS and GMM-IMM-LS algorithm, the localization error reached a value of approximately 0.61 m, 0.41 m, and 0.39 m, respectively, as the cumulative distribution probability was 90%; that for TSML, GMM-TSML and GMM-IMM-TSML were 0.55 m, 0.52 m, and 0.43 m, respectively; that for EKF, GMM-EKF and GMM-IMM-EKF were 0.58 m, 0.53 m, and 0.3 m, respectively. Apparently, the positioning algorithms under the framework of GMM-IMM outperformed the GMM-based algorithm and direct localization algorithms, and the GMM-IMM-EKF localization algorithm was superior to the other proposed algorithms. In other words, the GMM-IMM-EKF technique was able to achieve higher positioning accuracy in comparison with all localization algorithms and the position of the target node can be estimated with relatively

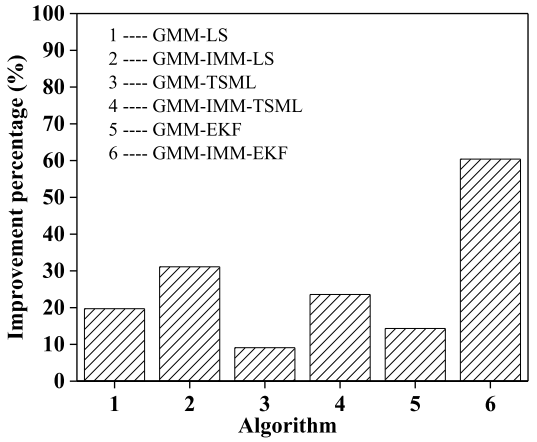

FIGURE 16. The improvement percentage of the average localization error relative to the corresponding single positioning algorithms.

high accuracy for the underground mine environment in LOS/NLOS/LOS-NLOS transition situations.

To have a better comparison of the mentioned localization algorithms, the more detailed statistical localization errors with respect to the maximum, minimum, average, and standard deviation of localization error were summarized in Table 1. According to these outcomes, it was observed that LS, TSML and EKF approaches under the framework of GMM-IMM was able to achieve the lowest average localization error, indicating that both GMM and IMM made a tremendous contribution to distance reconstruction and the positioning accuracy was significantly ameliorated. As expected, the proposed GMM-IMM-EKF technique with the lowest average localization error and standard deviation exhibited the more excellent localization performance than the compared methods, which was 0.1883 m and 0.0722 m, respectively, demonstrating that the GMM-IMM-EKF method was more robust than other approaches

To further investigate the performance of the enhancement of GMM-based approach and GMM-IMM-based algorithm comprehensively, we calculated the improvement percentage of the average localization error relative to the corresponding single positioning algorithm, as depicted in Fig.16. It was straightforward to see that the positioning accuracy of the GMM-LS, GMM-TSML, and GMM-EKF were improved by 19.71%, 9.12%, and 14.34% on average localization error compared with LS, TSML, and EKF, respectively, that for GMM-IMM-LS, GMM-IMM-TSML, and GMM-IMM-EKF were improved by 32.12%, 23.58%, and 60.41%, respectively. Undoubtedly, the GMM-IMM-EKF approach significantly enhanced the localization accuracy compared with the other approaches. The outstanding performance of the proposed GMM-IMM-EKF technique was mainly due to the smoothing of the measurement data and the mitigation of the adverse effects of NLOS biases by both the GMM-IMM and EKF in the mentioned approach, which was propitious to achieve higher accuracy than other positioning methods.

TABLE 1. Comparison localization error (m).

Algorithm	Maximum	Minimum	Average	Deviation
LS	0.6455	0.2139	0.3541	0.1276
GMM-LS	0.5231	0.1681	0.2843	0.0873
GMM-IMM-LS	0.4205	0.1589	0.2439	0.0755
TSML	0.6129	0.2033	0.3803	0.1289
GMM-TSML	0.5655	0.1505	0.3456	0.1328
GMM-IMM-TSML	0.4917	0.1442	0.2906	0.1112
EKF	0.6202	0.3470	0.4756	0.0855
GMM-EKF	0.5693	0.3107	0.4074	0.0786
GMM-IMM-EKF	0.3811	0.0828	0.1883	0.0722

VII. CONCLUSION

In this paper, to enhance positioning accuracy for complicate underground environment in mixed LOS/NLOS/LOS-NLOS scenarios, a novel approach GMM-IMM-EKF was proposed. By adopting GMM algorithm to eliminate the effect of LOSNLOS situation and two parallel self-adjusting VBAKFs under the framework of IMM technique to alleviate the LOS and NLOS errors, respectively, the measured distances between target node and corresponding AN can be more accurately re-estimated for frequent transitions between LOS, NLOS, and LOS-NLOS situation. Then, with the smoothed result of IMM-VBAKF, the EKF approach was utilized to estimate the location of the target node. The experimental verification demonstrated that GMM-based localization algorithm performed better than that of the corresponding single-model, and the positioning accuracy was significantly further enhanced by exploiting GMM-IMM-based methods. Furthermore, the proposed GMM-IMM-EKF algorithm, showing the highest improvement percentage of the average localization and providing the lowest localization error as compared with the other approaches, exhibited the best positioning performance, which can effectively eliminate the interference of severe NLOS errors and achieve higher positioning accuracy in LOS/NLOS/LOS-NLOS transition conditions. For near future research, we intend to further ameliorate and evaluate the reliability of the GMM-IMMEKF algorithm in terms of localization accuracy, enabling it apply to the underground harsh environment.

REFERENCES

[1] S. K. Michael and D. W. Hainsworth, "Outcomes of the landmark longwall automation project with reference to ground control issues," in *Proc. 24th Int. Conf. Ground Control Mining*, Oct. 2005, pp. 66–73.

[2] G. A. Einicke, J. C. Ralston, C. Hargrave, D. C. Reid, and D. W. Hainsworth, "Longwall mining automation an application of minimum-variance smoothing," *IEEE Control Syst. Mag.*, vol. 28, no. 6, pp. 28–37, Dec. 2008.

[3] S. Hao, S. Wang, R. Malekian, B. Zhang, W. Liu, and Z. Li, "A geometry surveying model and instrument of a scraper conveyor in unmanned longwall mining faces," *IEEE Access*, vol. 5, pp. 4095–4103, 2017.

[4] W. Shibo, Z. Boyuan, W. Shijia, and G. Shirong, "Dynamic precise positioning method of shearer based on closing path optimal estimation model," *IEEE Trans. Autom. Sci. Eng.*, vol. 16, no. 3, pp. 1468–1475, Jul. 2019.

[5] S. S. Ghassemzadeh, R. Jana, C. W. Rice, W. Turin, and V. Tarokh, "Measurement and modeling of an ultra-wide bandwidth indoor channel," *IEEE Trans. Commun.*, vol. 52, no. 10, pp. 1786–1796, Oct. 2004.
[6] H. Yang, T. Luo, W. Li, L. Li, Y. Rao, and C. Luo, "A stable SINS/UWB integrated positioning method of shearer based on the multi-model intelligent switching algorithm," *IEEE Access*, vol. 7, pp. 29128–29138, 2019.
[7] Y. Qin, F. Wang, and C. Zhou, "A distributed UWB-based localization system in underground mines," *J. Netw.*, vol. 10, no. 3, pp. 134–140, Mar. 2015.
[8] W. Xie, X. Li, and X. Long, "Underground operator monitoring platform based on ultra-wide band WSN," *Int. J. Online Eng.*, vol. 14, no. 10, pp. 219–229, 2018.
[9] Q. Fan, W. Li, J. Hui, L. Wu, Z. Yu, W. Yan, and L. Zhou, "Integrated positioning for coal mining machinery in enclosed underground mine based on SINS/WSN," *Sci. World J.*, vol. 2014, pp. 1–12, Jan. 2014.
[10] J. Schroeder, S. Galler, K. Kyamakya, and K. Jobmann, "NLOS detection algorithms for ultra-wideband localization," in *Proc. 4th Workshop Positioning, Navigat. Commun.*, Mar. 2007, pp. 159–166.
[11] S. Gezici, H. Kobayashi, and H. V. Poor, "Nonparametric nonline-of-sight identification," in *Proc. IEEE 58th Veh. Technol. Conf. (VTC -Fall)*, vol. 4, Oct. 2003, pp. 2544–2548.
[12] I. Guvenc, C.-C. Chong, and F. Watanabe, "NLOS identification and mitigation for UWB localization systems," in *Proc. IEEE Wireless Commun. Netw. Conf.*, Mar. 2007, pp. 1571–1576.
[13] S. Venkatesh and R. M. Buehrer, "Non-line-of-sight identification in ultra-wideband systems based on received signal statistics," *IET Microw., Antennas Propag.*, vol. 1, no. 6, pp. 1120–1130, Dec. 2007.
[14] H. Shimizu, H. Masui, M. M. Ishii, and K. Sakawa, "LOS and NLOS pathloss and delay characteristics at 3.35 GHz in a residential environment," *EICE Trans. Fundam. Electron. Commun. Comput. Sci.*, vol. 83, no. 7, pp. 1356–1364, Jul. 2000.
[15] P.-C. Chen, "A non-line-of-sight error mitigation algorithm in location estimation," in *Proc. WCNC. IEEE Wireless Commun. Netw. Conf.*, Sep. 1999, pp. 316–320.
[16] K. Yu and Y. J. Guo, "NLOS error mitigation for mobile location estimation in wireless networks," in *Proc. IEEE 65th Veh. Technol. Conf. (VTC-Spring)*, Apr. 2007, pp. 1071–1075.
[17] X.-H. Li and T. Zhang, "Research on improved UWB localization algorithm in NLOS environment," in *Proc. Int. Conf. Intell. Transp., Big Data Smart City (ICITBS)*, Jan. 2018, pp. 707–711.
[18] E. Garcia, P. Poudereux, Á. Hernández, J. Urena, and D. Gualda, "A robust UWB indoor positioning system for highly complex environments," in *Proc. IEEE Int. Conf. Ind. Technol. (ICIT)*, Mar. 2015, pp. 3386–3391.
[19] S. Xiaoqiang, L. K. Le, and C. Xi, "A method of TOA positioning for mine to effectively reduce the impact of non–line of sight error propagation," in *Proc. Chin. Control Decis. Conf. (CCDC)*, Jun. 2018, pp. 4650–4655.
[20] Q. Wang, I. Balasingham, M. Zhang, and X. Huang, "Improving RSS-based ranging in LOS-NLOS scenario using GMMs," *IEEE Commun. Lett.*, vol. 15, no. 10, pp. 1065–1067, Oct. 2011.
[21] G. Qing, K. Wei, and T. Wanchun, "Wireless positioning method based on dynamic objective function under mixed LOS/NLOS conditions," in *Proc. Ubiquitous Positioning, Indoor Navigat. (UPINLBS)*, Mar. 2018, pp. 1–4.
[22] Y. Zhang, Y. Zhu, F. Yan, Z. Li, and L. Shen, "Non-line-of-sight mitigation in wireless localization and tracking via semidefinite programming," in *Proc. IEEE 27th Annu. Int. Symp. Pers., Indoor, Mobile Radio Commun. (PIMRC)*, Sep. 2016, pp. 1–6.
[23] A. Ribeiro, I. D. Schizas, S. Roumeliotis, and G. B. Giannakis, "Kalman filtering in wireless sensor networks," *IEEE Control Syst.*, vol. 30, no. 2, pp. 66–86, Apr. 2010.
[24] C.-H. Park and J.-H. Chang, "Robust LMedS-based WLS and Tukey-based EKF algorithms under LOS/NLOS mixture conditions," *IEEE Access*, vol. 7, pp. 148198–148207, 2019.
[25] W. Liu, T. Liu, and L. Tang, "Indoor localization algorithm based on particle filter optimization in NLOS environment," in *Proc. Int. Conf. Commun. Signal Process. Syst.*, vol. 516, Aug. 2018, pp. 1143–1148.
[26] J. Wang, T. Zhang, X. Xu, and Y. Li, "A variational Bayesian based strong tracking interpolatory cubature Kalman filter for maneuvering target tracking," *IEEE Access*, vol. 6, pp. 52544–52560, 2018.
[27] M. Y. Fu, Z. H. Deng, and J. W. Zhang, *Kalman Filtering Theory and Its Application in Navigation System*. Beijing, China: Science Press, 2001.
[28] D. M. Blei, A. Kucukelbir, and J. D. McAuliffe, "Variational inference: A review for statisticians," *J. Amer. Stat. Assoc.*, vol. 112, no. 518, pp. 859–877, Apr. 2017.
[29] S. Sarkka and A. Nummenmaa, "Recursive noise adaptive Kalman filtering by variational Bayesian approximations," *IEEE Trans. Autom. Control*, vol. 54, no. 3, pp. 596–600, Mar. 2009.
[30] S.-Y. Wang, C. Yin, S.-K. Duan, and L.-D. Wang, "A modified variational Bayesian noise adaptive Kalman filter," *Circuits, Syst., Signal Process.*, vol. 36, no. 10, pp. 4260–4277, Oct. 2017.
[31] Y.-Y. Huang, Y.-W. Jing, and Y.-B. ShI, "Non-parametric mobile node localization for IOT by variational Bayesian approximations adaptive Kalman filter," *Cognit. Syst. Res.*, vol. 52, pp. 27–35, Dec. 2018.
[32] H. A. P. Blom and Y. Bar-Shalom, "The interacting multiple model algorithm for systems with Markovian switching coefficients," *IEEE Trans. Autom. Control*, vol. 33, no. 8, pp. 780–783, Aug. 1988.
[33] K. Yoo, J. Chun, and J. Shin, "Target tracking and classification for missile using interacting multiple model (IMM)," in *Proc. Int. Conf. Radar (RADAR)*, Aug. 2018, pp. 1–6.
[34] L. Xiang and Y. Zhou, "Consensus on IMM-UKFs for tracking in mixed LOS/NLOS conditions," in *Proc. Chin. Control Conf. (CCC)*, Jul. 2019, pp. 4427–4432.
[35] B.-S. Chen, C.-Y. Yang, F.-K. Liao, and J.-F. Liao, "Mobile location estimator in a rough wireless environment using extended Kalman-based IMM and data fusion," *IEEE Trans. Veh. Technol.*, vol. 58, no. 3, pp. 1157–1169, Mar. 2009.
[36] Y. Zhang, W. Fu, D. Wei, J. Jiang, and B. Yang, "Moving target localization in indoor wireless sensor networks mixed with LOS/NLOS situations," *EURASIP J. Wireless Commun. Netw.*, vol. 2013, no. 1, p. 291, Dec. 2013.
[37] D.-C. Chang and M.-W. Fang, "Bearing-only maneuvering mobile tracking with nonlinear filtering algorithms in wireless sensor networks," *IEEE Syst. J.*, vol. 8, no. 1, pp. 160–170, Mar. 2014.
[38] C. Fritsche, U. Hammes, A. Klein, and A. M. Zoubir, "Robust mobile terminal tracking in NLOS environments using interacting multiple model algorithm," in *Proc. IEEE Int. Conf. Acoust., Speech Signal Process.*, Apr. 2009, pp. 3049–3052.
[39] J. Borras, P. Hatrack, and N. B. Mandayam, "Decision theoretic framework for NLOS identification," *Proc. 48th IEEE Veh. Technol. Conf.*, vol. 2, May 1998, pp. 1583–1587.
[40] B. Guermah, T. Sadiki, and H. E. Ghazi, "Improving vehicle localization in hard environment using GNSS-GSM hybridization and Gaussian mixture noise," in *Proc. Int. Conf. Control, Autom. Diagnosis (ICCAD)*, Mar. 2018, pp. 1–6.
[41] V. Melnykov and I. Melnykov, "Initializing the EM algorithm in Gaussian mixture models with an unknown number of components," *Comput. Statist. Data Anal.*, vol. 56, no. 6, pp. 1381–1395, Jun. 2012.
[42] J. A. Hartigan and M. A. Wong, "Algorithm AS 136: A K-means clustering algorithm," *J. Roy. Stat. Soc. C, Appl. Stat.*, vol. 28, no. 1, pp. 100–108, 1979.
[43] R. Weinstock, *Calculus of Variations: With Applications to Physics and Engineering*. New York, NY, USA: Dover, 1974.
[44] Y. T. Chan and K. C. Ho, "A simple and efficient estimator for hyperbolic location," *IEEE Trans. Signal Process.*, vol. 42, no. 8, pp. 1905–1915, Aug. 1994.
[45] S. Monica and F. Bergenti, "Hybrid indoor localization using WiFi and UWB technologies," *Electronics*, vol. 8, no. 3, p. 334, Mar. 2019.
[46] G. Shen, R. Zetik, and R. S. Thoma, "Performance comparison of TOA and TDOA based location estimation algorithms in LOS environment," in *Proc. 5th Workshop Positioning, Navigat. Commun.*, Mar. 2008, pp. 71–78.
[47] B. Cao, S. Wang, S. Ge, W. Liu, S. Wang, and S. Yi, "Study on the improvement of ultra-wideband localization accuracy in narrow and long space," *Sensor Rev.*, vol. 40, no. 1, pp. 42–53, Nov. 2019.
[48] L. Cheng, S. C. Fi, P. J. Wang, S. J. Chen, C. Liu, K. Zong, and M. Wu, "Base station layout analysis of UWB pose detection for roadheader based on Chan algorithm," (in Chinese), *Coal Technol.*, vol. 37, no. 8, pp. 278–280, Aug. 2018.

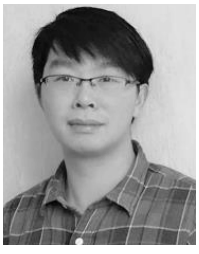

BO CAO received the M.S. degree in mechanical design and theory from the China University of Mining and Technology, Xuzhou, China, in 2015, where he is currently pursuing the Ph.D. degree in mechanical design and theory.

His current research interests include wireless sensor networks, UWB deployment, improvement positioning accuracy, underground localization and navigation, and machine learning.

SHIBO WANG received the Ph.D. degree in mechanical design and theory from the China University of Mining and Technology, Xuzhou, China, in 2007.

He is currently a Professor with the China University of Mining and Technology. His current research interests include tribology, principles of intelligent perception of mining equipment, mechanism of hard rock cutting, and robotic mining technology. He has won one Second Prize for scientific and technological progress of the Ministry of Education and one First Prize for science and technology of Chinese Machinery Industry.

SHIRONG GE received the Ph.D. degree in mechanical engineering from the China University of Mining and Technology, Xuzhou, China, in 1989.

He is currently a Professor and the Deputy Secretary of the Party Committee of the China University of Mining and Technology at Beijing. His research interests include biological tribology, tribology nonlinear theory, disaster relief robot and mining machinery reliability, and other scientific research. He has been appointed as a member of the Fifth Science and Technology Committee of the Ministry of Education and the Ninth and Tenth Expert Evaluation Team of the Ministry of Engineering and Materials Science of the National Natural Science Foundation of China. He is a member of the Academic Committee of the State Key Laboratory of Tribology, Tsinghua University, the State Key Laboratory of Solid Lubrication, Chinese Academy of Sciences, and the State Key Laboratory of Mechanical Transmission, Chongqing University. He has won two National Second Prizes for technological invention and one National Second Prize for scientific and technological progress. He is the Vice-Chairman of the China Coal Society and the Chairman of the China Institute of Mechanical Engineering Friction Branch.

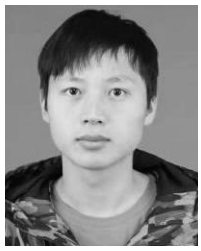

XIUZE MA is currently pursuing the master's degree with the School of Mechanical and Electrical Engineering, China University of Mining and Technology, Xuzhou, China.

His research interests include mining machinery, coal seam modeling, coal seam modeling, and intelligent mining equipment.

WANLI LIU received the Ph.D. degree from Tianjin University, Tianjin, China, in 2016.

He is currently a Researcher with the Jiangsu Collaborative Innovation Center of Intelligent Mining Equipment, China University of Mining and Technology, Xuzhou, China. His research interests include mobile laser scanning, accuracy improvement light detection and ranging, inertial measurement unit, and underground position and navigation.